ELSEVIER

Journal of Hazardous Materials 141 (2007) 622–629

Journal of Hazardous Materials

www.elsevier.com/locate/jhazmat

# Simultaneous uptake of ammonium and phosphate ions by compounds prepared from paper sludge ash

Kiyoshi Okada [a,*], Yosuke Ono [a,1], Yoshikazu Kameshima [a], Akira Nakajima [a], Kenneth J.D. MacKenzie [b]

[a] *Department of Metallurgy and Ceramics Science, Tokyo Institute of Technology, O-okayama, Meguro, Tokyo 152-8552, Japan*
[b] *School of Chemical and Physical Sciences, Victoria University of Wellington, P.O. Box 600, Wellington, New Zealand*

Received 7 January 2006; received in revised form 9 May 2006; accepted 11 July 2006
Available online 14 July 2006

**Abstract**

Al-containing $CaO–SiO_2–H_2O$ phases were prepared by hydrothermal treatment of mixtures of paper sludge ash (PSA) with various silica and calcia sources and their properties were determined with particular reference to the simultaneous uptake of ammonium and phosphate ions, which are implicated in the eutrophication of lakes and ponds. After examination of various silica and calcia sources, $Ca(OH)_2$ and $SiO_2$ sol were selected as the most appropriate starting materials. Dry milling was found to be superior to wet milling in avoiding contamination from the milling media during mixing. Nine samples with three different Ca/Si ratios and $Al_2O_3$ contents were prepared with various mass ratios of $Ca(OH)_2$, PSA and $SiO_2$. The chemical compositions of the hydrothermal products of these mixtures moved towards the tieline of $CaSiO_3$-PSA, with respect to the starting compositions. The major phase formed in all samples was poorly crystalline C–S–H(I), with hydroxysodalite also formed in the Al-containing mixtures. All the products showed a capacity for the simultaneous uptake of ammonium and phosphate ions. The saturated sorption capacities calculated from the Langmuir equation ranged from 0.9 to 2.4 mmol/g for the ammonium ion and from 3.3 to 5.2 mmol/g for the phosphate ion. Since the sorption capacities for both ions increased with increasing Ca contents of the product, substitution of $Ca^{2+}$ for $NH_4^+$ and the formation of calcium phosphate phases such as apatite and brushite by precipitation are thought to be the main sorption mechanisms.


*Keywords:* Paper sludge ash; $CaO–SiO_2–H_2O$ phase; Simultaneous uptake; Eutrophication; Ammonium ion; Phosphate ion

## 1. Introduction

The vast amount of paper used in everyday life generates a large amount of waste, 50–60% of which is recycled. The unrecycled waste is heat-treated and the ash buried in landfills. The main constituents of paper sludge waste are cellulose fibers ($[C_6H_{10}O_5]_n$) and the ceramic powders used as fillers and coating materials. The latter are mainly kaolinite ($Al_2Si_2O_5(OH)_4$), calcite ($CaCO_3$) and talc ($Mg_3Si_4O_{10}(OH)_2$). As one possible method for re-using this waste, we have produced activated carbon from old paper by chemical and physical activation methods [1]. The resulting chemically activated products show excellent sorption capability, and the physically activated products retain the original paper shape even after activation [2,3].

The main chemical constituents of PSA are CaO, $Al_2O_3$ and $SiO_2$. Since these are combinations of basic, amphoteric and acidic components, paper sludge is expected to have multi-functional sorption properties after it has been appropriately heat-treated to develop an active phase for sorption. We have previously found that amorphous $CaAl_2Si_2O_8$ prepared by calcining 1:1 mixtures of kaolinite and calcite shows high and selective uptake properties for heavy metal ions [4]. This observation led us to heat-treat paper sludge at 500–1000 °C and examine its sorption of heavy metal ions [5]. The amorphous $CaO–Al_2O_3–SiO_2$ (CAS) prepared by calcining paper sludge at 600–800 °C was found to show good sorption capacity for both phosphate ions and heavy metal ions [6].

The $CaO–SiO_2–H_2O$ system contains many different calcium silicate hydrates which can be synthesized by hydrothermal treatment [7]. Tobermorite ($Ca_5Si_6H_2O_{18}·4H_2O$), one of the

* Corresponding author. Tel.: +81 3 5734 2524; fax: +81 3 5734 3355.
*E-mail address:* kokada@ceram.titech.ac.jp (K. Okada).
[1] Present address: Asahi Kasei Chemicals, Yako, Kawasaki, Kanagawa 210-0863, Japan.

0304-3894/$ – see front matter © 2006 Elsevier B.V. All rights reserved.
doi:10.1016/j.jhazmat.2006.07.017

better-known calcium silicate hydrates, exists with a range of Ca/Si ratios from 0.8 to 1.0 due to its chemically flexible layer structure. Al substitution for Si is also known to occur in tobermorite. Ma et al. [8] prepared Al-substituted tobermorite from coal fly ash under mild hydrothermal conditions and reported that the Al substitution conferred excellent selective uptake properties for Cs and Sr. Recently, Coleman [9] prepared a similar phase from stoichiometrically adjusted mixtures of recycled newsprint waste, sodium silicate and calcia under hydrothermal conditions at 100 °C. Changing the Ca/Si ratio from the ideal value of 5/6 and/or increasing the degree of Al-substitution lowers the crystallinity of the tobermorite, which is then better described as $CaO–SiO_2–H_2O$ gel (C–S–H). In terms of the applications of these materials as adsorbents, C–S–H gel is probably preferable to tobermorite because of its higher specific surface area and its formation with a wider range of Ca/Si ratios and Al-substitution.

We therefore consider that the synthesis of Al-substituted C–S–H gel from paper sludge ash (PSA) is a potentially useful method for reusing paper waste. This work describes the preparation of Al-substituted CSH gels from mixtures of PSA, silica and calcia sources under mild hydrothermal conditions and the investigation of their ability to simultaneously sorb ammonium and phosphate ions, which are implicated in environmental eutrophication problems.

## 2. Experimental

### 2.1. Sample preparation

PSA was supplied by the Fuji Paper Making Union, Fuji, Japan. The other chemical reagents ($SiO_2$ gel, $SiO_2$ sol, $Ca(OH)_2$ and $CaCO_3$) were used supplied by Kanto Chemicals, Japan. The experimental flow chart describing the sample preparation procedure is shown in Fig. 1. The starting materials were mixed in the mass ratios $CaO:PSA:SiO_2 = 1:x:y$, where $x = 0$, 1 and 2, and $y = 1$, 2 and 4. A total of 3.0 g of each composition was prepared. In the preliminary experiments, four samples were prepared using combinations of each of the two silica and calcia sources to determine the most appropriate starting reagents. Mixing was carried out under both wet and dry conditions in an $Al_2O_3$ pot (80 ml) with 300 $Al_2O_3$ balls (Ø5 mm) using a planetary ball mill (LAPO.1, Ito, Japan), expecting some mechanochemical reaction during the mixing.

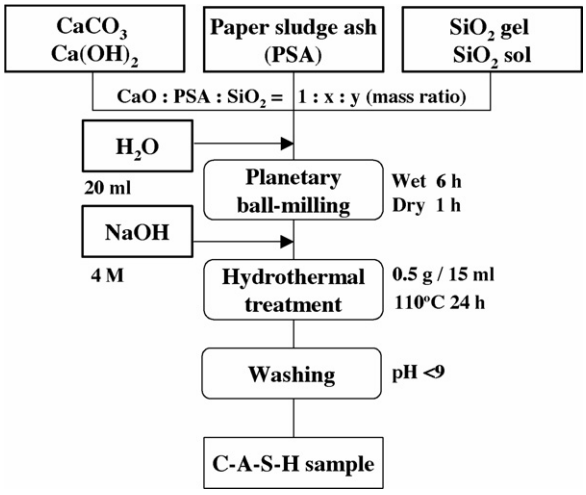


Fig. 1. Experimental flow scheme for the preparation of the present samples.

Hydrothermal synthesis was performed in a 25 ml Teflon-lined autoclave. 0.5 g samples were reacted in 15 ml of 4 M NaOH solution at 110 °C for 24 h. After reaction, the product was washed with distilled water until the pH of the washed solution was 9. The solid was then centrifuged and dried at 110 °C in an oven overnight.

### 2.2. Simultaneous sorption experiments

The simultaneous sorption of ammonium and phosphate ions was investigated under the following conditions; temperature: 25 °C, sample/solution ratio: 0.3 g/25 ml, initial concentration of ammonium and phosphate ions (from $NH_4H_2PO_4$ solution): 0.01–100 mM, reaction time: 24 h. The pH values were measured immediately prior to placing the sample into the solution (recorded as the initial pH) and after the reaction (recorded as the final pH). After the uptake experiments, the samples were filtered, washed three times with distilled water and dried at 110 °C overnight. The separated solutions were chemically analyzed for $Ca^{2+}$, $Na^+$, $Al^{3+}$ and $Si^{4+}$ by ICP-OES (Leeman Labs Inc., USA). The ammonium and phosphate ion concentrations were measured by ion chromatography (IA-200, DKK·TOA, Japan). Agreement in the results of triplicate measurements was better than 5%.

### 2.3. Characterization

The bulk chemical composition of the samples before and after hydrothermal synthesis was determined by X-ray fluorescence (RIX2000, Rigaku, Japan). The resulting crystalline phases were identified by powder X-ray diffraction (XRD) using an XRD-6100 diffractometer (Shimadzu, Japan) with monochromated Cu Kα radiation. Solid-state $^{29}Si$ and $^{27}Al$ MAS NMR spectra were obtained at 11.7 T using a Varian Unity 500 spectrometer and a Doty probe spun at 10–12 kHz. The $^{29}Si$ spectra were acquired using a 90° pulse of 60 μs and a recycle delay time of 100 s, and were referenced to tetramethylsilane (TMS). The $^{27}Al$ spectra were acquired using a 15° pulse of 1 μs and a recycle delay time of 1 s and were referenced to $Al(H_2O)_6^{3+}$. The specific surface area was calculated by the BET method from the $N_2$ isotherms determined using an automatic gas adsorption instrument (Autosorb-1, Quanta Chrome, USA). The sample was preheated at 180 °C for 1 day under vacuum condition before the measurement.

## 3. Results and discussion

### 3.1. Preparation and characterization of the samples

Samples of composition $CaO:PSA:SiO_2 = 1:2:2$ were prepared using various combinations of each of the calcia and

Table 1
Chemical compositions and specific surface areas of the starting materials and products after hydrothermal treatment

| Sample | $SiO_2$ | $Al_2O_3$ | CaO | MgO | $Na_2O$ | Others[a] | $S_{BET}$ ($m^2$/g) |
|---|---|---|---|---|---|---|---|
| PSA | 34.1 | 28.3 | 26.5 | 7.8 | 0.0 | 3.3 | – |
| No. 1 (101) | 48.5 | 0.2 | 50.7 | 0.2 | 0.1 | 0.3 | – |
| No. 2 (111) | 42.7 | 7.6 | 46.7 | 1.9 | 0.1 | 1.0 | – |
| No. 3 (121) | 42.0 | 11.7 | 41.3 | 2.8 | 0.2 | 2.0 | – |
| No. 4 (102) | 65.1 | 0.3 | 34.0 | 0.0 | 0.0 | 0.6 | – |
| No. 5 (112) | 59.0 | 5.3 | 33.3 | 1.3 | 0.2 | 0.9 | – |
| No. 6 (122) | 53.7 | 9.4 | 32.5 | 2.3 | 0.2 | 1.9 | – |
| No. 7 (104) | 78.1 | 0.4 | 20.5 | 0.2 | 0.3 | 0.7 | – |
| No. 8 (114) | 72.2 | 3.6 | 22.2 | 1.0 | 0.3 | 0.7 | – |
| No. 9 (124) | 67.7 | 6.7 | 22.9 | 1.7 | 0.3 | 0.7 | – |
| No. 1H (101) | 50.7 | 0.3 | 48.5 | 0.4 | 0.0 | 0.1 | 100 |
| No. 2H (111) | 46.0 | 7.7 | 43.5 | 2.0 | 0.2 | 0.6 | 250 |
| No. 3H (121) | 42.5 | 11.2 | 40.9 | 3.1 | 0.5 | 1.9 | 280 |
| No. 4H (102) | 56.3 | 0.2 | 43.2 | 0.3 | 0.0 | 0.0 | 240 |
| No. 5H (112) | 52.9 | 6.2 | 37.6 | 1.7 | 0.4 | 1.3 | 230 |
| No. 6H (122) | 49.8 | 10.4 | 34.3 | 2.8 | 0.7 | 2.0 | 200 |
| No. 7H (104) | 57.0 | 0.3 | 42.4 | 0.2 | 0.0 | 0.1 | 180 |
| No. 8H (114) | 53.7 | 7.0 | 35.5 | 1.9 | 0.3 | 1.6 | 240 |
| No. 9H (124) | 52.2 | 10.4 | 30.5 | 2.5 | 0.8 | 3.5 | 170 |

[a] $TiO_2$, $Fe_2O_3$, $P_2O_5$, and $K_2O$.

silica sources $Ca(OH)_2$, $CaCO_3$, $SiO_2$ sol and $SiO_2$ gel. After hydrothermal treatment, the phases formed in all these samples were C–S–H(I) (the major phase) and hydroxysodalite ($Na_8Al_6Si_6O_{24}(OH)_2$) (the minor phase). In addition, small amounts of katoite ($Ca_3Al_2SiO_4(OH)_8$) and/or gehlenite ($Ca_2Al_2SiO_7$) were observed in all the samples except for that produced from $Ca(OH)_2$ and $SiO_2$ sol; this combination was therefore used in all the subsequent experiments.

Samples containing CaO, PSA and $SiO_2$ in the ratio of 1:0:2, 1:1:2 and 1:2:2 were mixed using a planetary ball mill under both wet and dry conditions. Chemical analysis of the wet and dry-milled samples showed that the $Al_2O_3$ content of the wet-milled samples was always 3–6 mass% higher than that of the dry-milled samples. A considerable amount of $Al_2O_3$ (about 6 mass%) was detected in the wet-milled samples containing no $Al_2O_3$ in the starting material, suggesting that $Al_2O_3$ contamination is introduced from the milling media in the wet-milling process. By contrast, only a small amount of $Al_2O_3$ (0.3 mass%) was detected in the dry-milled samples, leading to the adoption of dry milling as the standard process for sample preparation.

The chemical compositions of the nine samples before and after hydrothermal reaction are shown in Table 1 and Fig. 2. The chemical compositions are clearly changed by the hydrothermal reaction, moving closer to the tieline of $CaSiO_3$-PSA. This trend leads to especially large changes in the silica-rich samples (Nos. 7, 8 and 9), and suggests that the products of hydrothermal synthesis have Ca/Si ratios of approximately unity.

The XRD patterns of the hydrothermally reacted samples are shown in Fig. 3. All the samples show diffraction peaks of C–S–H(I) with the ideal composition $Ca_5Si_5O_{15}\cdot 6H_2O$ [10]. By contrast, hydroxysodalite is also formed in the Al-containing samples (Nos. 5H, 6H, 8H, and 9H). A small amount of calcite also detected in sample No. 1, which has the highest CaO content. The change in chemical composition after hydrothermal synthesis is thus attributable to the formation of C–S–H(I) as the major phase.

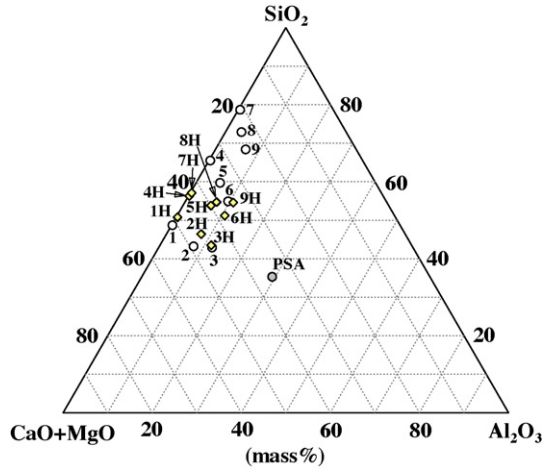


Fig. 2. Chemical composition of the samples before and after hydrothermal reaction. Key—open circles: before reaction; open diamonds: after reaction.

The specific surface areas of the samples after hydrothermal reaction are listed in Table 1. Most of the samples except No. 1 (101) show specific surface areas of 200–300 $m^2$/g. These values are similar to that of C–S–H(I) synthesized by hydrothermal treatment of diatomite with $Ca(OH)_2$ in NaOH solution [11].

The $^{29}Si$ and $^{27}Al$ MAS NMR spectra of the samples are shown in Fig. 4(a) and (b), respectively. All the $^{29}Si$ MAS NMR spectra are quite similar and show a clear peak at −83

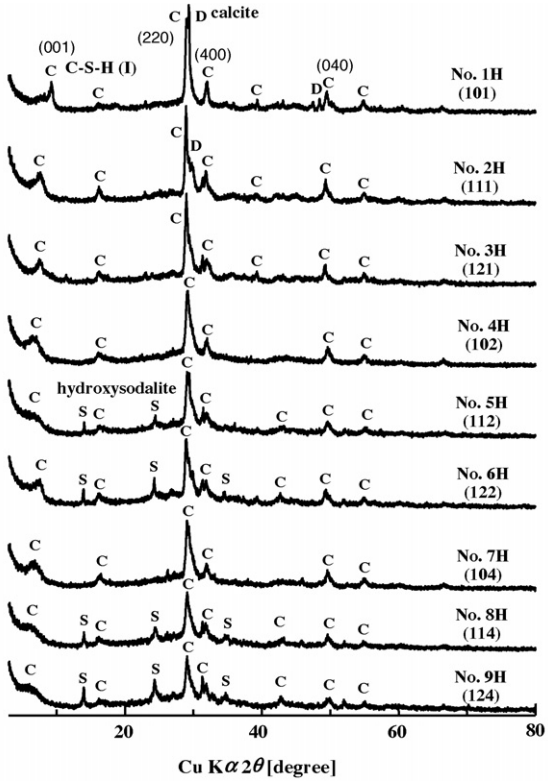


Fig. 3. XRD patterns of the hydrothermally reacted materials.

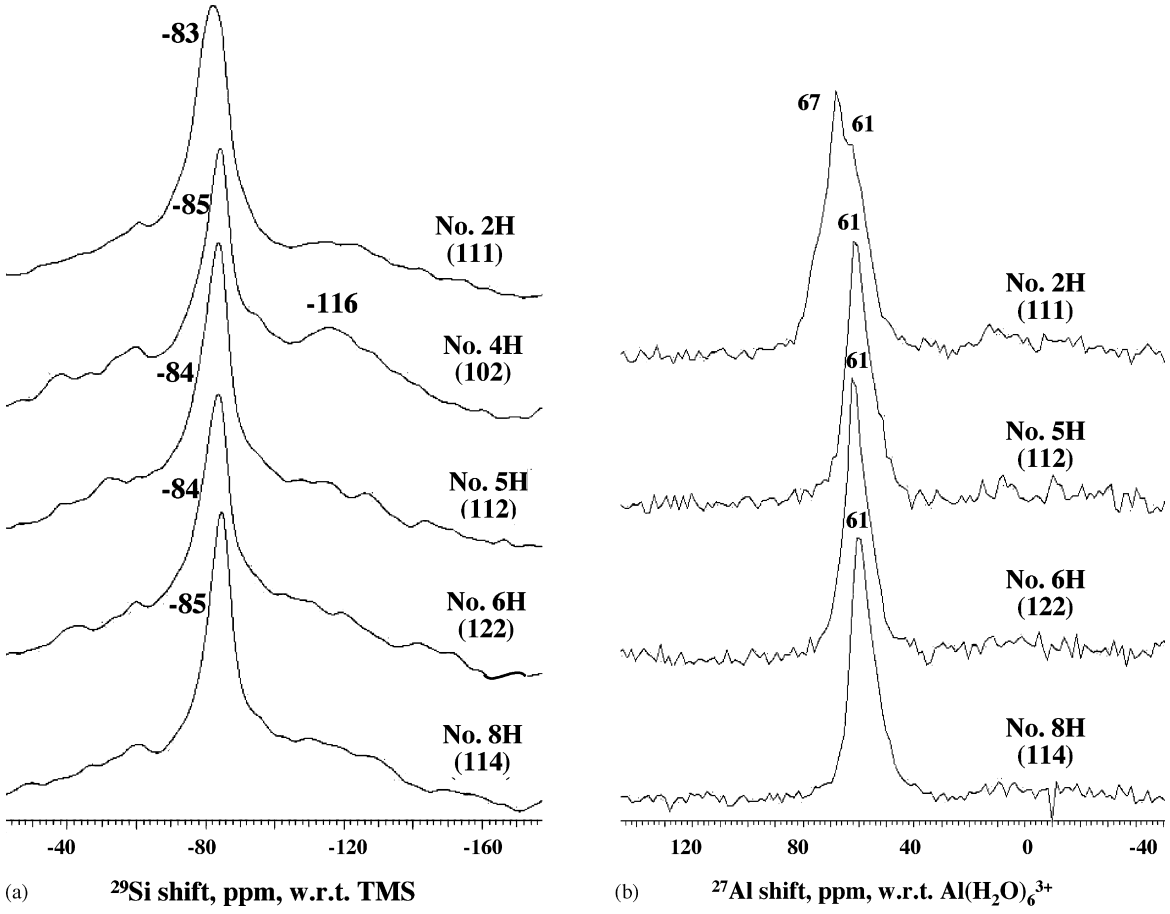


Fig. 4. $^{29}$Si (a) and $^{27}$Al (b) MAS NMR spectra of the samples after hydrothermal reaction.

to −85 ppm, irrespective of the Ca/Si ratio and Al content. A broad peak is also observed at −116 ppm in sample No. 4H, assigned to a framework structure. Coleman [9] reported the assignment of $^{29}$Si MAS NMR of Al-substituted tobermorites as follows: $Q^1$ at −81.4 ppm arising from breaks in the aluminosilicate chains, $Q^2$(1Al) at −83.5 ppm, assigned to the mid-chain, $Q^2$(0Al) at −86.5 ppm, assigned to the silicate tetrahedra of the wollastonite-like alumino-silicate chains, and $Q^3$(1Al) at −93.5 ppm, assigned to bridging silicate tetrahedra. The peaks at −83 to −85 ppm in the present samples are therefore assigned to the overlapping peaks of the $Q^2$(1Al) and $Q^2$(0Al) units. The poor resolution of these two peaks suggests that the phase in the samples is C–S–H(I) rather than tobermorite. The $^{27}$Al MAS NMR spectra show a clear peak at 61 ppm arising from Al in tetrahedral coordination. Sample No. 2H shows an additional peak at 67 ppm, suggesting the presence of two slightly different local arrangements around the $AlO_4$ tetrahedra.

The particle shapes of the three samples, Nos. 3H, 6H and 9H, are shown by SEM to all adopt a platy morphology but with different particle sizes, decreasing with increasing silica content from samples 9H to 6H to 3H. The edges of the particles in sample No. 3H are curled due to the thinness of the plates. This particle shape is very different from the lath-shaped particles observed in Al-substituted tobermorite [8,9] (Fig. 5).

### 3.2. Simultaneous sorption of ammonium and phosphate ions

The ammonium and phosphate sorption isotherms for samples 4H, 5H and 6H are shown in Fig. 6(a) and (b), respectively. These data were fitted by the least-squares method using the Langmuir (1) and Freundlich (2) equations are shown below:

$$Q_e = \frac{Q_0 b C_e}{1 + bC_e} \quad (1)$$

$$Q_e = K C_e^{1/n} \quad (2)$$

where $Q_e$ (mmol/g) and $C_e$ (mmol/l) are the equilibrium phosphate adsorption and concentration, $Q_0$ (mmol/g) the maximum monolayer adsorption capacity, $b$ the Langmuir constant (l/mmol), and $K$ (mmol/g) and $n$ are the Freundlich constants. The calculated results for the nine samples are listed in Table 2, which also shows the correlation coefficients ($r$). The resulting $r$ values show slightly better fits to the Freundlich equation than the Langmuir equation for the ammonium sorption isotherms, but the phosphate isotherms are better fitted by the Langmuir equation than the Freundlich equation. The shapes of the isotherms (Fig. 6) and the saturated sorption values suggest that the phosphate ion has a higher affinity for these sorbents

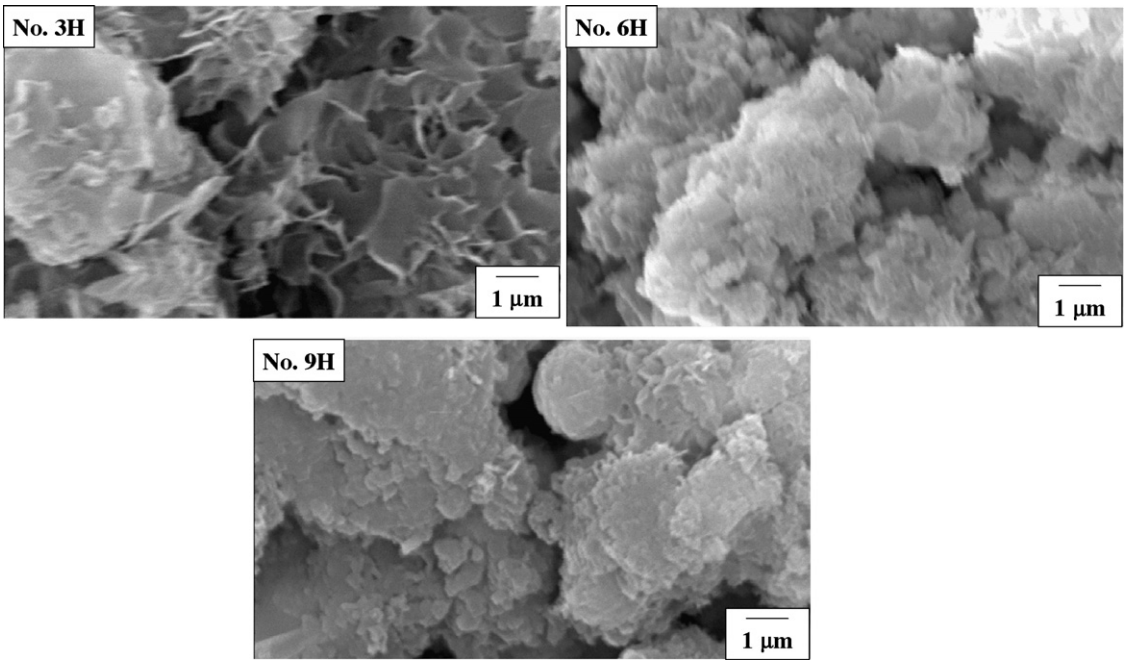


Fig. 5. SEM micrographs of the samples after hydrothermal reaction.

than the ammonium ion. This is reflected by the sorption energy ($\Delta G$) (Table 1), determined from the equation $\Delta G = -RT\ln(b)$, where $R$ is the gas constant. The $\Delta G$ values for the ammonium ion range from −5.8 to −10.5 kJ/mol while those for the phosphate ion range from −9.3 to −16.0 kJ/mol. The absolute values of the ammonium sorption energy in these samples are of similar magnitude to energies of physical sorption (several kJ/mol). The negative values of $\Delta G$ indicate that sorption of ammonium and phosphate ions occurs spontaneously on these sorbents.

To examine the simultaneous sorption mechanisms of ammonium and phosphate ions on the present samples, the post-sorption samples were characterized by XRD and MAS NMR spectroscopy. The XRD patterns of the samples after the sorption experiments (Nos. 4HU and 5HU) are shown in Fig. 7(a) and (b), respectively. Both samples show little change after sorption at initial concentrations of ammonium and phosphate ions up to 10 mM, but hydroxyapatite ($Ca_5(PO_4)_3(OH)$) is observed in both samples at ion concentrations greater than 30 mM. At 100 mM, strong XRD peaks of brushite ($CaHPO_4{\cdot}2H_2O$) are clearly observed, in addition to hydroxyapatite peaks in sample No. 5HU, but no brushite peaks occur in sample No. 4HU. Hydroxyapatite is the only other phase observed in all the other samples which do not contain PSA while brushite is clearly observed in all the samples containing PSA, exposed to ionic concentrations of 100 mM. Since there are no significant differences in the final pH or maximum adsorption of both types of samples, the Al component appears to play an important role in the precipitation of calcium phosphate phases. The samples in which calcium phosphates are formed show phosphate

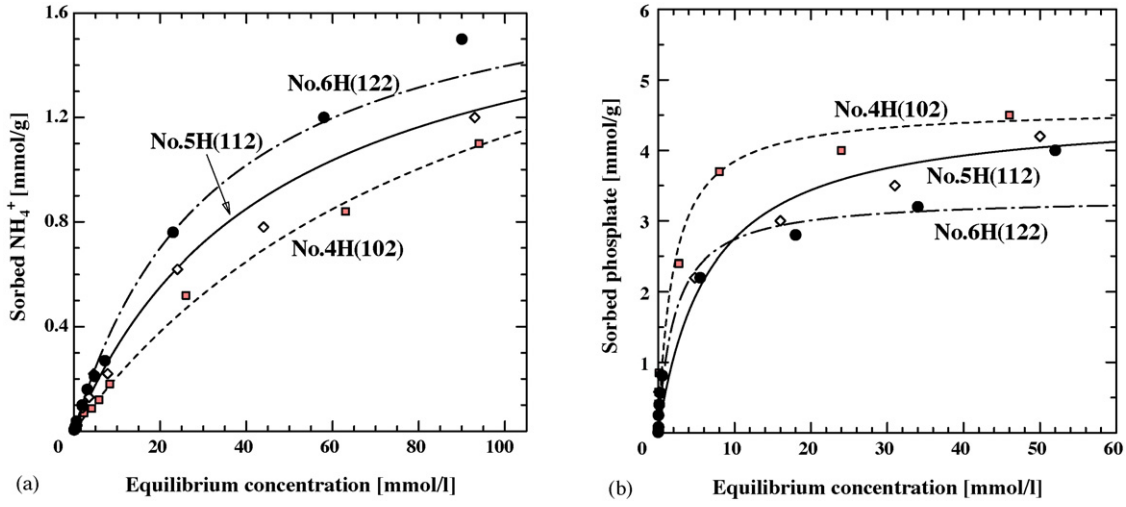


Fig. 6. Sorption isotherms of samples 4H, 5H and 6H for (a) ammonium ions; (b) phosphate ions.

Table 2
Langmuir and Freundlich parameters of ammonium and phosphate sorption

| Sample | Langmuir parameter | | | | Freundlich parameter | | | Sorbate |
|---|---|---|---|---|---|---|---|---|
| | $Q_0$ (mmol/g) | $b$ (l/mmol) | $\Delta G$ (kJ/mol) | $r$ | $K$ (mmol/g) | $n$ | $r$ | |
| No. 1H (101) | 2.02 | 0.013 | −10.7 | 0.7662 | 0.025 | 1.07 | 0.9874 | Ammonium |
| No. 2H (111) | 2.36 | 0.027 | −8.9 | 0.9591 | 0.030 | 1.01 | 0.9972 | Ammonium |
| No. 3H (121) | 2.14 | 0.063 | −6.9 | 0.9965 | 0.038 | 1.03 | 0.9781 | Ammonium |
| No. 4H (102) | 2.21 | 0.010 | −11.3 | 0.9868 | 0.026 | 1.15 | 0.9959 | Ammonium |
| No. 5H (112) | 1.84 | 0.021 | −9.5 | 0.9284 | 0.039 | 1.19 | 0.9896 | Ammonium |
| No. 6H (122) | 1.86 | 0.030 | −8.7 | 0.9403 | 0.058 | 1.30 | 0.9968 | Ammonium |
| No. 7H (104) | 1.05 | 0.030 | −8.7 | 0.9820 | 0.027 | 1.18 | 0.9859 | Ammonium |
| No. 8H (114) | 0.90 | 0.070 | −6.6 | 0.9873 | 0.054 | 1.45 | 0.9842 | Ammonium |
| No. 9H (124) | 1.47 | 0.042 | −7.8 | 0.9760 | 0.058 | 1.34 | 0.9940 | Ammonium |
| No. 1H (101) | 5.15 | 0.422 | −2.1 | 0.9880 | 0.560 | 1.59 | 0.7147 | Phosphate |
| No. 2H (111) | 4.91 | 0.539 | −1.5 | 0.9935 | 1.063 | 1.65 | 0.9262 | Phosphate |
| No. 3H (121) | 4.68 | 0.425 | −2.1 | 0.9724 | 0.504 | 1.59 | 0.9228 | Phosphate |
| No. 4H (102) | 4.61 | 0.502 | −1.7 | 0.9934 | 0.924 | 1.68 | 0.8808 | Phosphate |
| No. 5H (112) | 4.58 | 0.150 | −4.7 | 0.9943 | 0.689 | 1.67 | 0.9101 | Phosphate |
| No. 6H (122) | 3.34 | 0.458 | −1.9 | 0.9943 | 0.592 | 1.65 | 0.9177 | Phosphate |
| No. 7H (104) | 4.60 | 0.639 | −1.1 | 0.9942 | 1.085 | 2.20 | 0.9048 | Phosphate |
| No. 8H (114) | 3.44 | 0.644 | −1.1 | 0.9967 | 0.746 | 1.93 | 0.9766 | Phosphate |
| No. 9H (124) | 3.68 | 0.335 | −2.7 | 0.9961 | 0.581 | 1.73 | 0.9840 | Phosphate |

sorption >2 mmol/g; this higher phosphate sorption is therefore attributed to the precipitation of calcium phosphate by reaction of $Ca^{2+}$ dissolved from the samples, with the phosphate in solution. By contrast, the initial stage of phosphate uptake is thought to be due to an adsorption mechanism because the sample surfaces are positively charged at the initial pH values of 4–6. As $Ca^{2+}$ is dissolved from the samples, the solution pH increases and ammonium ion sorption occurs by substitution of $Ca^{2+}$ for $NH_4^+$ and adsorption on the negatively charged surfaces of the samples.

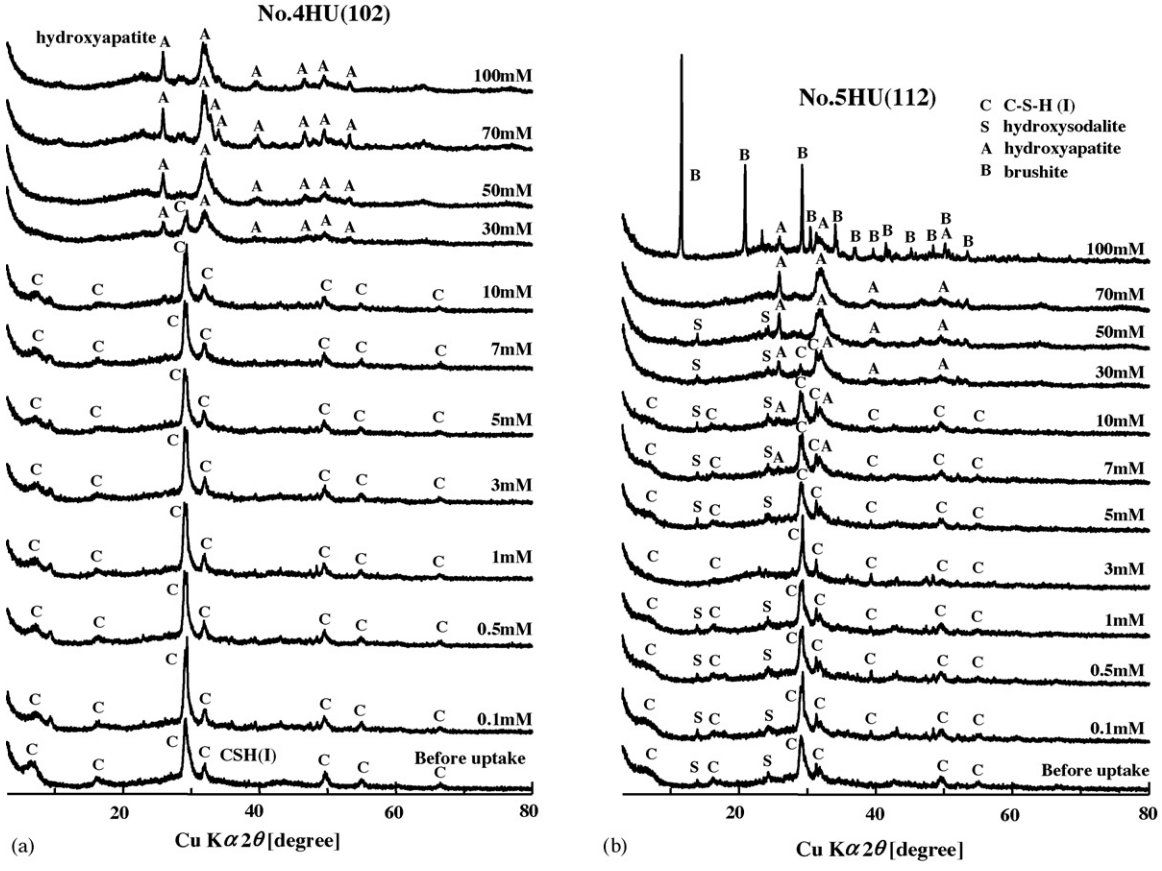


Fig. 7. XRD patterns of (a) sample 4H and (b) sample 5H after the sorption experiments carried out with various initial ionic concentrations.

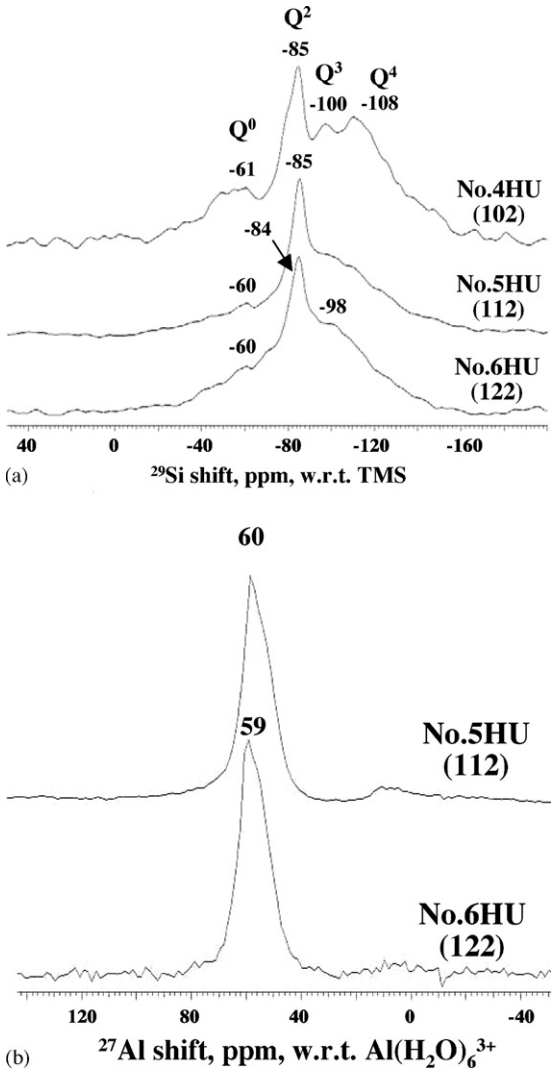


Fig. 8. (a) $^{29}$Si and (b) $^{27}$Al MAS NMR spectra of the samples after the sorption experiment.

The $^{29}$Si and $^{27}$Al MAS NMR spectra of the samples after the uptake experiments at an initial concentration of 10 mM are shown in Fig. 8(a) and (b), respectively. Although these samples show little change in the XRD patterns after the sorption experiments (Fig. 7), the $^{29}$Si spectra show the appearance of a resonance at −98 ppm corresponding to a $Q^3$ species, by contrast with the spectra of the same samples before the sorption experiments (Fig. 4). The new resonance is attributed to the structure change associated with polymerization of $SiO_4$ tetrahedra by partial dissolution of $Ca^{2+}$ from the samples, and is seen most clearly in sample No. 4 in which there is no Al-substitution.

At the start of this study, we assumed that Al-substitution in the calcium silicate hydrate phases would enhance the sorption capability because of the presence of locally unbalanced electrostatic charges. However, no clear relationship was observed between the $Al_2O_3$ content of the samples and the sorption of ammonium and phosphate ions. By contrast, a clear trend of increasing sorption of ammonium and phosphate ions with increasing (CaO + MgO) content was found (Fig. 9). It is therefore concluded that dissolution of $Ca^{2+}$ from the samples is an important factor in the uptake of ammonium ions by adsorption and ion-replacement mechanisms, whereas adsorption and calcium precipitation are the predominant mechanisms for phosphate ion uptake from solution.

The capability of various materials for simultaneous sorption of ammonium and phosphate ions [6,12–15] is summarized in Fig. 10. The previously reported data, lying in the range shown by the straight lines, represent a trade-off; materials showing high ammonium sorption, e.g. sepiolite [15] and $Al_2O_3$/potassium aluminosilicate (KAS) [12] show rather low phosphate sorption while those showing high phosphate sorption, e.g. PSA [6] and steel making slag (SMS) [13] show low ammonium sorption. By contrast, the present materials show higher phosphate sorption than SMS, in addition to usefully high ammonium sorption. It is therefore clear that the present materials have much better simultaneous sorption capability for ammonium and phosphate than any previously reported materials. Of the present nine samples, Nos. 1–5 show particularly

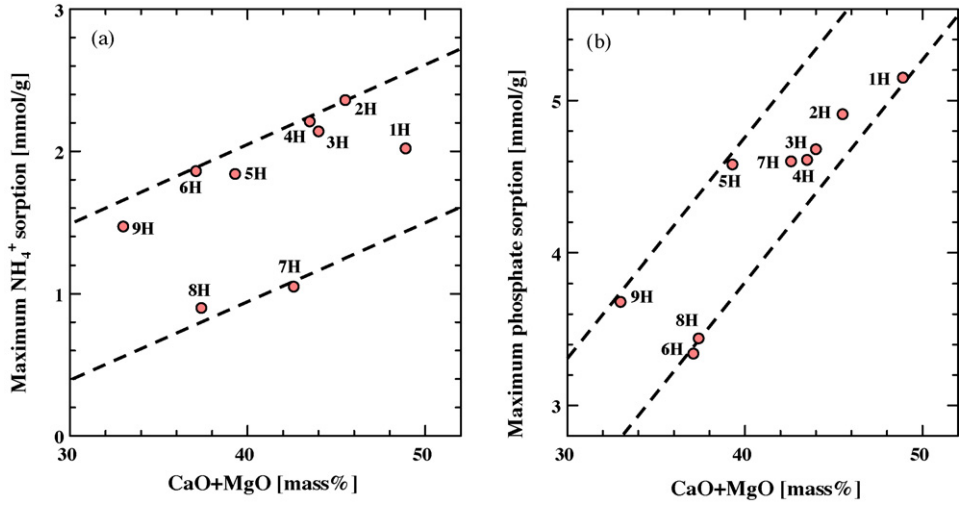


Fig. 9. Relationship between the (CaO + MgO) content of the samples and the maximum sorption capacities for (a) ammonium ions and (b) phosphate ions.

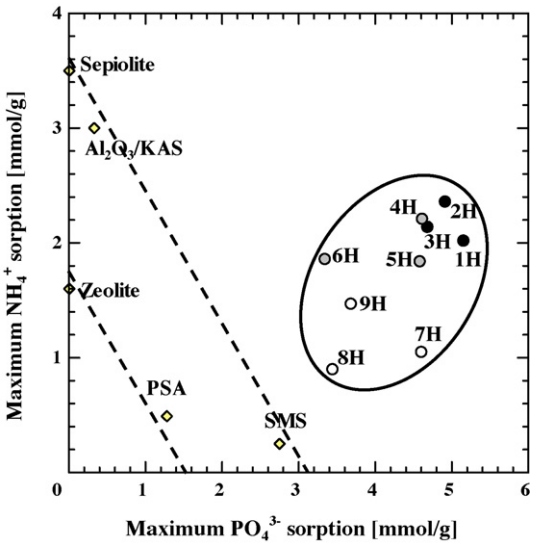


Fig. 10. Comparison of simultaneous sorption capacity for ammonium and phosphate ions of the present samples with the previously reported materials (PSA [6], $Al_2O_3$/KAS [12], SMS [13], zeolite [14] and sepiolite [15]).

promising sorption properties. Although the sorption abilities of the present samples are considered to be influenced by co-presenting various cations and anions in the water, the effects were found to be less strong in the compounds having similar uptake mechanisms with the present samples than in the ion-exchange type compounds, e.g. zeolites [4]. Thus, we think that the present samples with higher sorption abilities are suitable materials for simultaneous uptake of ammonium and phosphate ions in sewage.

## 4. Conclusion

Poorly crystalline $CaO–SiO_2–H_2O$ (C–S–H) and Al-containing C–S–H phases were hydrothermally synthesized from mixtures of paper sludge ash, calcia and silica in NaOH solution, and their simultaneous sorption of the eutrophication-related ions, ammonium and phosphate, was investigated. The following results were obtained:

(1) $Ca(OH)_2$, $SiO_2$ sol and PSA are the best starting materials to synthesize monophasic Al-containing C–S–H.
(2) The main product is C–S–H(I), with the ideal chemical composition $Ca_5Si_5O_{15}·6H_2O$. The resulting particles had a fine, platy shape and specific surface area of 200–300 $m^2/g$.
(3) All the samples showed excellent simultaneous sorption abilities for ammonium and phosphate ions. The isotherms were best fitted by the Freundlich equation for ammonium ion adsorption but the Langmuir equation gave the best fit for phosphate ion adsorption.
(4) The saturated sorption amounts of ammonium and phosphate ions ranged from 0.9 to 2.4 mmol/g and from 3.3 to 5.2 mmol/g, respectively. The sorption ability increases with increasing (CaO + MgO) content of the samples.
(5) The simultaneous sorption abilities for ammonium and phosphate ions in the present materials are much better than for previously reported materials.

## References

[1] K. Okada, N. Yamamoto, Y. Kameshima, A. Yasumori, Preparation of activated carbon from waste newspaper by chemical and physical activations, J. Colloid Interf. Sci. 262 (2003) 179–193.
[2] K. Okada, N. Yamamoto, Y. Kameshima, A. Yasumori, Adsorption properties of activated carbons prepared from waste newspaper by chemical and physical activation, J. Colloid Interf. Sci. 262 (2003) 194–199.
[3] K. Okada, Y. Shimizu, Y. Kameshima, A. Nakajima, Preparation and properties of carbon/zeolite composites with corrugate structure, J. Porous Mater. 12 (2005) 289–299.
[4] K. Okada, N. Watanabe, V.K. Jha, Y. Kameshima, A. Yasumori, K.J.D. MacKenzie, Uptake of various cations by amorphous $CaAl_2Si_2O_8$ prepared by solid-state reaction of kaolinite with $CaCO_3$, J. Mater. Chem. 12 (2003) 550–556.
[5] V.K. Jha, Y. Kameshima, A. Nakajima, K. Okada, K.J.D. MacKenzie, Effect of grinding and heating on $Ni^{2+}$ uptake properties of waste paper sludge, J. Environ. Manage. 80 (2006) 363–371.
[6] V.K. Jha, Y. Kameshima, A. Nakajima, K. Okada, K.J.D. MacKenzie, Multifunctional uptake behaviour of materials prepared by calcining Waste Paper Sludge, J. Environ. Sci. Health 41 (2006) 703–719.
[7] L. Black, K. Garbev, P. Stemmermann, K.R. Hallam, G.C. Allen, X-ray photoelectron study of oxygen bonding in crystalline C–S–H phases, Phys. Chem. Miner. 31 (2004) 337–346.
[8] W. Ma, P.W. Brown, S. Komarneni, Sequestration of cesium and strontium by tobermorite synthesized from fly ashes, J. Am. Ceram. Soc. 79 (1996) 1707–1710.
[9] N.J. Coleman, Synthesis, structure and ion exchange properties of 11 Å tobermorites from newsprint recycling residue, Mater. Res. Bull. 40 (2005) 2000–2013.
[10] K. Mohon, H.F.W. Taylor, A trimethylsilylation study of tricalcium silicate pastes, Cement Concr. Res. 12 (1982) 25–31.
[11] G.G. Martirosyan, A.G. Manukyan, K.A. Kostanyan, Study of filtration and adsorption properties of calcium hydrometasilicate, Russ. J. Appl. Chem. 75 (2002) 209–212.
[12] K. Okada, J. Temuujin, Y. Kameshima, K.J.D. MacKenzie, Simultaneous uptake of ammonium and phosphate ions by composites of γ-alumina/potassium aluminosilicate gel, Mater. Res. Bull. 38 (2003) 749–756.
[13] V.K. Jha, Y. Kameshima, A. Nakajima, K. Okada, Hazardous ions uptake behavior of thermally activated steel-making slag, J. Hazard. Mater. B 114 (2004) 139–144.
[14] M. Rozic, S. Cerjan-Stefanovic, S. Kurajica, V. Vancina, E. Hodzic, Ammoniacal nitrogen removal from water by treatment with clays and zeolites, Water Res. 34 (2000) 3675–3681.
[15] S. Balci, Y. Dincel, Ammonium ion adsorption with sepiolite: use of transient uptake method, Chem. Eng. Process. 41 (2002) 79–85.